



Research article

Exploring the effect of NK-cell related molecules on the prognosis and tumor microenvironment of gastric cancer patients: Evidence from large sample populations

Yuqin Li^{a,1}, Dejun Wu^{b,c,1}, Anjun Xu^{b,c,1}, Ming Xu^{b,c}, Baiqing Fu^{a,**},
Wujun Xiong^{a,*}

^a Department of Gastroenterology, Shanghai Pudong Hospital, Fudan University Pudong Medical Center, 2800 Gongwei Road, Pudong New District, Shanghai, 201399, China

^b Department of General Surgery, Shanghai Pudong Hospital, Fudan University Pudong Medical Center, 2800 Gongwei Road, Shanghai, 201399, China

^c Department of Gastrointestinal Surgery, Shanghai Pudong Hospital, Fudan University Pudong Medical Center, 2800 Gongwei Road, Shanghai, 201399, China

A B S T R A C T

Background: Natural killer (NK) cells play a significant role in anti-tumor immunity, and their involvement has been documented in various cancers. However, a deeper understanding of the mechanisms by which NK cells influence gastric cancer progression remains necessary.

Methods: We utilized the Cancer Genome Atlas (TCGA) database to acquire transcriptional profiles, clinical information, and mutation data for gastric cancer patients. R software and associated packages were employed for all analyses of this publicly available data.

Results: We used multiple algorithms to evaluate the tumor microenvironment in gastric cancer samples. We performed differential expression analysis to pinpoint genes related to NK cells. Utilizing this data, we developed a prognostic model featuring three crucial NK cell-related genes: MAB21L2, ARPP21, and MUCL1. This model showed strong predictive performance in the training and validation groups. Consistently, patients identified as high-risk according to our model had worse overall survival rates. To further elucidate the biological differences between high-risk and low-risk patients, we performed enrichment analyses focusing on biological pathways and immune-related factors. Additionally, we observed a correlation between higher risk scores and non-responsiveness to treatment. Interestingly, high-risk patients were found to be potentially more sensitive to axitinib. We selected MUCL1 for further investigation due to its potential role in the model. While MUCL1 mRNA levels were elevated in both gastric cancer and paired normal tissues, protein expression analysis using the Human Protein Atlas database revealed a decrease in MUCL1 protein levels within tumor tissues.

Conclusions: Our findings contribute to a more comprehensive understanding of the role of NK cells in gastric cancer and highlight MUCL1 as a promising therapeutic target.

1. Introduction

Gastric cancer is a leading cause of global cancer deaths, with particularly high incidence and mortality rates in East Asia [1]. Its pathogenesis is complex, involving factors such as *Helicobacter pylori* infection, unhealthy dietary habits, and genetic and environmental influences [2]. Despite the use of surgery, radiotherapy, and chemotherapy as standard-of-care treatment, the five-year survival

* Corresponding author.

** Corresponding author.

E-mail addresses: kfyfbq@sina.com (B. Fu), xiongwujun@126.com (W. Xiong).

¹ These authors contributed equally to this work.

rate for gastric cancer remains low [3]. Advancements in molecular biology and cancer genomics have paved the way for targeted therapy as a novel approach to gastric cancer management [4]. Compared with conventional chemotherapy, targeted therapies act on specific molecular abnormalities within cancer cells, leading to potentially improved efficacy and reduced side effects on healthy cells [5]. Several targeted drugs, like the HER2 antibody Trastuzumab and the multi-target tyrosine kinase inhibitor Ramucirumab, have already received clinical approval for gastric cancer treatment [6,7]. It is widely thought that the future of gastric cancer treatment lies in the integration of novel targeted therapies with immunotherapies, offering more personalized and effective treatment options. Checkpoint inhibitors, a type of immunotherapy, hold promise for improving patient outcomes [8,9]. However, due to the inherent complexity and heterogeneity of gastric cancer, research continues to focus on identifying new therapeutic targets and developing even more targeted drugs [10].

Natural killer (NK) cells are crucial components of the innate immune system, recognizing and eliminating compromised cells, particularly cancerous and virus-infected ones [11]. Their activation and functional state significantly impact the suppression of tumor development and spread within the tumor's immune microenvironment [12]. However, many tumors, including gastric cancer, have evolved mechanisms to suppress NK cell activity, evading immune system clearance [13]. With a deepened understanding of the immune system's role in tumor development in recent years, the role of NK cells in gastric cancer immunosurveillance and treatment has gained significant attention [14,15]. Recent research has revealed multiple mechanisms by which NK cells recognize and eliminate gastric cancer cells. This includes the ability of NK cell surface receptors, such as NKG2D and Nkp30, to recognize specific markers on these cancer cells [16,17]. This finding provides a theoretical foundation for developing novel immunotherapeutic strategies. However, studies have also shown that gastric cancer cells can evade NK cell-mediated killing by expressing inhibitory molecules like MHC class I molecules, highlighting the complexity of tumor immune escape mechanisms [18]. Conversely, preclinical studies demonstrate the potential of novel immunomodulators, such as antibodies blocking inhibitory receptors on NK cells, to enhance their killing ability against gastric cancer cells [19]. Most importantly, cell-based therapies using NK cells, including NK cell transfer therapy and engineered NK cell therapy, have shown remarkable promise in improving treatment outcomes and survival rates for gastric cancer patients [20]. These advancements not only deepen our understanding of NK cells' role in the immune response to gastric cancer but also offer new avenues for treating this disease.

We employed various algorithms to assess the tumor microenvironment of gastric cancer tissues. Differential gene expression analysis identified NK cell-related genes. From these results, we built a prognostic model that included three important genes associated with NK cells: MAB21L2, ARPP21, and MUCL1. The model proved to be highly accurate in predicting outcomes for both the training and validation groups. Patients deemed high-risk by our model showed lower overall survival rates, as anticipated. To further elucidate the biological differences between high-risk and low-risk patients, we performed enrichment analyses focusing on biological pathways and immune-related factors. Additionally, we observed a correlation between higher risk scores and non-responsiveness to treatment. Interestingly, high-risk patients may be more sensitive to axitinib. Finally, *MUCL1*, a gene identified by the model, was selected for further investigation.

2. Methods

2.1. Data download and summarization

Public gastric cancer transcriptome and clinical datasets were sourced from The Cancer Genome Atlas (TCGA) database, specifically TCGA-STAD (<https://portal.gdc.cancer.gov/>) [21]. We retrieved the raw transcript data in STAR-Counts format from the TCGA-GDC portal and converted these to Transcripts Per Million (TPM) using R software, preparing them for subsequent analysis. Genome annotations were performed using downloaded annotation files (GRCh38) from the Ensembl website (<https://www.ensembl.org/index.html>). Clinical data was downloaded in bcr-xml format. All data underwent preprocessing steps before analysis, including genome annotation, normalization, and log₂ transformation. We obtained single-cell gene expression data directly from the Tumor Immune Single-cell Hub 2 (TISCH2) project. The TISCH2 web portal allowed us to access the data and perform targeted analyses of single-cell transcripts for genes of interest. This direct querying approach facilitated the efficient extraction of data relevant to our study goals [22]. Representative immunohistochemical (IHC) images were retrieved directly from the Human Protein Atlas (HPA) database (<https://www.proteinatlas.org/>). The HPA online analysis tool enabled us to search for images by inputting specific genes of interest. The user-friendly interface facilitated image categorization; normal tissue images were selected from the "Tissue" tab, while tumor tissue images were chosen from the "Pathology" tab [23].

2.2. Tumor microenvironment quantification

To evaluate the extent of cell infiltration within the tumor microenvironment, we utilized transcriptional profiling data analyzed by several established computational algorithms [24–29]. These algorithms included QUANTISEQ for quantifying tumor-immune cell infiltrates, EPIC for estimating stromal and immune cell proportions, MCPCOUNTER for identifying major cell populations in heterogeneous tissues, CIBERSORT for characterizing cell composition based on gene expression profiles, XCELL for enhancing data with cell type-specific signals, and TIMER for estimating immune infiltrate abundance. Each algorithm employs unique statistical methods and reference gene sets, allowing for a detailed and accurate analysis of the cellular dynamics within the tumor environment. All algorithms utilize standardized expression profile data from gastric cancer patients as input.

2.3. Prognosis-related analysis

Patients with gastric cancer were evenly split into training and validation cohorts in a 1:1 ratio. A two-step process was utilized to identify prognostic factors associated with survival. Initially, a univariate Cox proportional hazards model assessed the influence of each factor on overall survival. Factors showing a statistically significant link (p -value < 0.05) were chosen for further examination. To address the high dimensionality and possible multicollinearity in the data, Least Absolute Shrinkage and Selection Operator (LASSO) regression was used to refine our selection of prognostic factors. LASSO regression is beneficial as it minimizes the risk of model overfitting through the penalization of the coefficients' absolute values. A multivariate Cox regression model was subsequently developed with the factors identified by the LASSO regression. This method allowed for the identification of independent prognostic factors and accounted for potential confounders. We calculated a risk score for each patient using a linear combination of the expressions of the selected genes, weighted by their coefficients derived from the Cox model, according to the formula: Risk score = Gene A * Coef A + ... + Gene X * Coef X. Based on these risk scores, patients were divided into different risk categories. Kaplan-Meier survival curves were plotted for each group, and differences in survival rates were analyzed using the log-rank test. Lastly, a receiver operating characteristic (ROC) curve was constructed to measure the predictive performance of the prognostic model, and the area under the curve (AUC) was calculated to evaluate the model's discriminative ability regarding different survival outcomes.

2.4. Biological enrichment

To perform biological enrichment analysis, we utilized both ClueGO and Gene Set Enrichment Analysis (GSEA) [30,31]. First, DEGs between high- and low-risk patient groups were uploaded to the STRING database to retrieve their associated protein-protein interaction networks. These networks were then integrated into Cytoscape software. ClueGO, a Cytoscape plugin, was employed to visualize the non-redundant biological terms associated with these gene clusters, providing a comprehensive overview of functionally grouped networks. Next, to assess whether predefined gene sets exhibited statistically significant differences between high- and low-risk patients, we employed GSEA. Hallmark, Gene Ontology (GO), and Kyoto Encyclopedia of Genes and Genomes (KEGG) gene sets were used in this analysis. GSEA involves the calculation of normalized enrichment scores (NES) that indicate the degree to which each gene set is overrepresented at the top or bottom of a ranked gene list. Permutation testing was performed to determine statistical significance.

2.5. Immune status and immunotherapy evaluation

Gene expression profile data was used to quantify the immune score, stromal score, and estimate score using the Estimate package. Next, the ssGSEA algorithm was used to measure the immune status of each sample, using predefined gene sets. Next, we evaluated potential immunotherapy response differences using Tumor Immune Dysfunction and Exclusion (TIDE) analysis [32]. TIDE analysis was performed through the online TIDE website (<http://tide.dfci.harvard.edu/>), with the standardized expression profile data serving as the input. The resulting TIDE score reflects the potential response of patients to immunotherapy. Specifically, patients with a TIDE score less than 0 were classified as immunotherapy responders, while those with a score greater than 0 were classified as non-responders.

2.6. Drug sensitivity and nomogram plot

Gastric cancer patients may benefit from personalized treatment regimens tailored to their specific needs. To identify effective targeted and chemotherapy treatments, we analyzed IC50 values for various drugs within the Genomics of Drug Sensitivity in Cancer (GDSC) database [33]. IC50 values were assessed based on patients' genomic features. Leveraging these findings, we developed a nomogram that integrates prognostic risk scores with key clinical characteristics of gastric cancer patients, including age, tumor stage, and genetic profiles. This tool is designed to predict individual patient outcomes and guide clinicians in making informed treatment decisions. By visually representing the impact of various risk factors on a patient's prognosis, the nomogram facilitates a personalized approach to cancer treatment.

2.7. Cell culture and cell lines

The gastric cancer cell lines AGS, HGC-27, MKN-28, and BGC-83, along with the non-cancerous gastric cell line GES-1, were grown in appropriate media enriched with 10 % fetal bovine serum (FBS) and 1 % penicillin-streptomycin. These cell lines were kept at 37 °C in a humid environment with 5 % CO₂.

2.8. Quantitative real-time PCR (qPCR)

Total RNA was isolated from gastric cancer cell lines utilizing TRIzol reagent as per the instructions provided by the manufacturer. This RNA was subsequently converted into cDNA using a reverse transcription kit. The expression of MUCL1 was measured through qRT-PCR, employing SYBR Green PCR master mix on a real-time PCR system. GAPDH served as the reference gene for normalizing expression levels. The primer used were: MUCL1, forward, 5'-TAGAGCTAGCGAATTATGAAGTTCTTAGCAGTCC-3'; reverse, 5'-AGATCCTTCGCGGCCTCAGGGACACACTCTACCA-3'; GAPDH, forward, 5'-CGCTGAGTACGTCGTGGAGTC-3'; reverse, 5'-

GCTGATGATCTTGAGGCTGTTGTC-3'.

2.9. Western blot analysis

Protein extracts were obtained from gastric cancer cell lines using RIPA buffer containing protease inhibitors. Protein levels were determined with a BCA Protein Assay Kit. Proteins were equally loaded and separated via SDS-PAGE, then transferred to PVDF membranes. These membranes were blocked using 5 % non-fat milk and probed with primary antibodies against MUCL1 (NBP1-92366; 1:500; Novus Biologicals, LLC) and GAPDH (60004-1-Ig, 1:10000, Proteintech). Following several washes, the membranes were treated with HRP-linked secondary antibodies. The protein bands were detected using enhanced chemiluminescence (ECL) reagents.

2.10. Cell transfection

Cells were transfected with MUCL1-specific siRNAs purchased from Santa Cruz Biotechnology (siRNA#1, siRNA#2) and a negative control siRNA using Lipofectamine 2000 according to the manufacturer's instructions. The efficiency of the knockdown was verified by qPCR analyses 48 h post-transfection.

2.11. Cell proliferation assay

The proliferation of gastric cancer cells post-siRNA transfection was evaluated using the Cell Counting Kit-8 (CCK-8). At specified

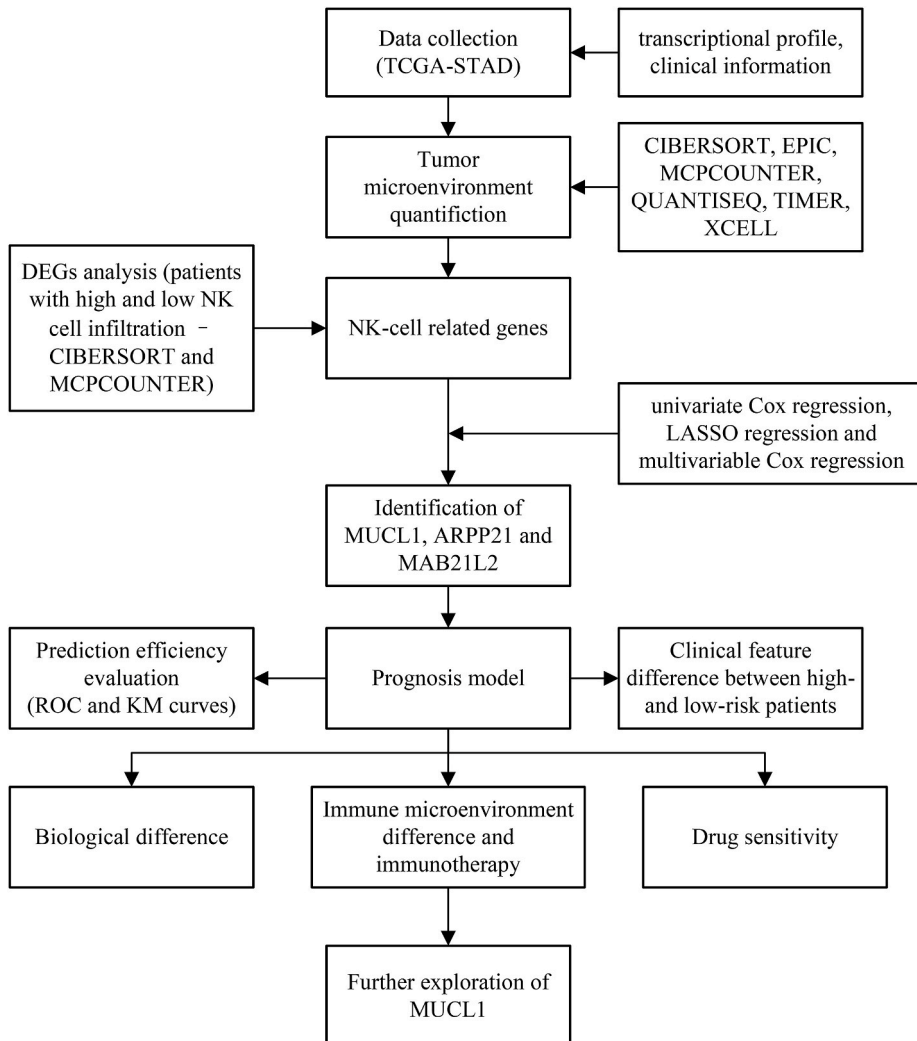


Fig. 1. The flow chart of whole study.

time points (0, 24, 48, 72h), CCK-8 solution was added to the cells, and absorbance was measured at 450 nm to determine cell viability.

2.12. Transwell assay

Cell migration was evaluated using a transwell migration assay. Twenty-four hours after siRNA transfection, gastric cancer cells were placed in the upper chamber of a Transwell insert (8 μm pore size) with serum-free medium. The lower chamber contained medium with 10 % fetal bovine serum to serve as a chemoattractant. Following a 24-h incubation at 37 °C, cells that had migrated to the lower surface of the membrane were fixed with 4 % paraformaldehyde and stained with 0.1 % crystal violet. The cells that crossed the membrane were examined and counted using a light microscope across five random fields per insert.

2.13. Statistical analysis

All statistical analyses were performed using the R programming language, a robust environment for data manipulation, statistical

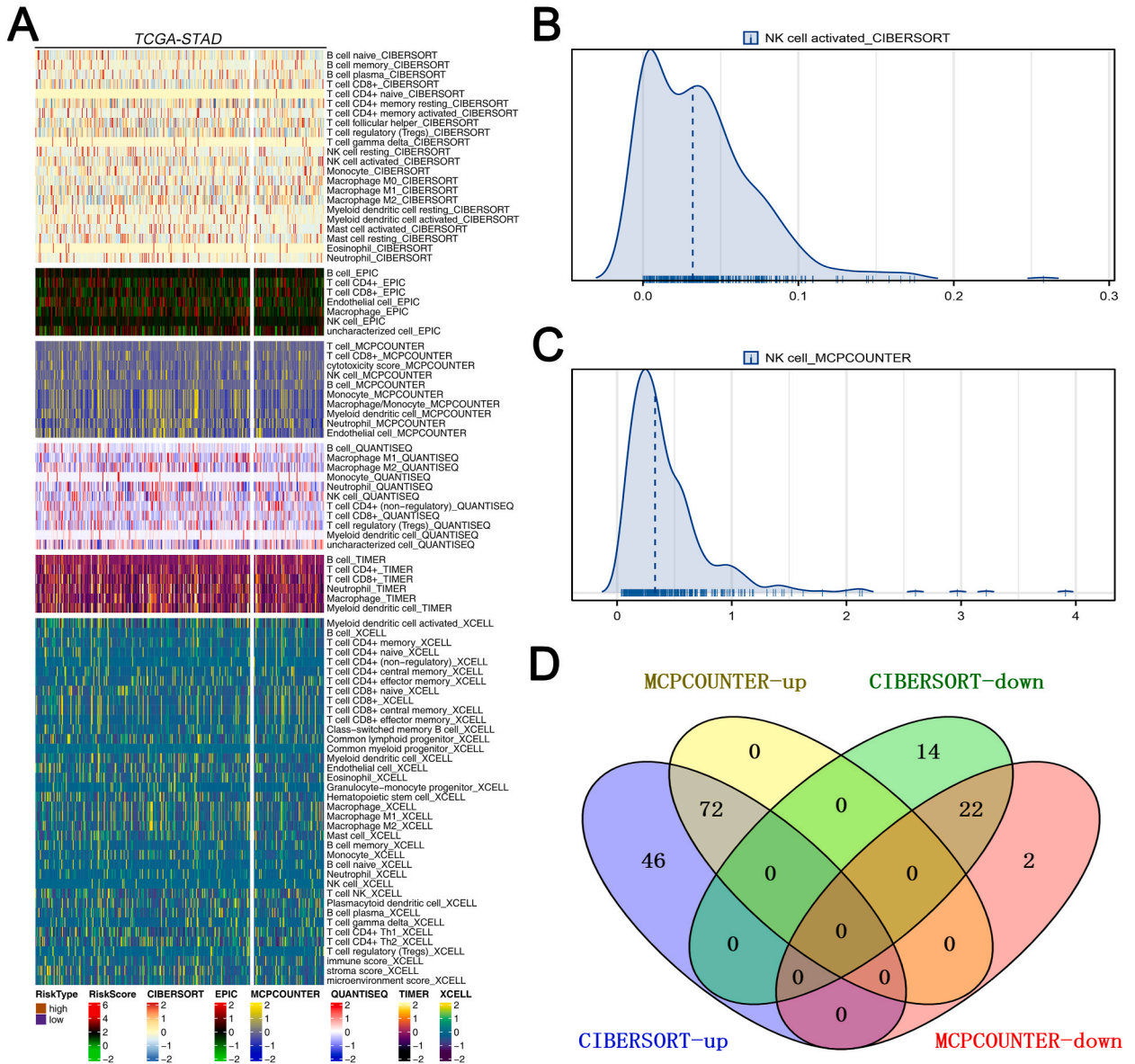


Fig. 2. The infiltration level of NK cells was quantified by multiple algorithms.

Notes: A: The tumor microenvironment was quantified by multiple algorithms; B: The immune infiltration level of NK cells quantified by CIBERSORT algorithm; C: The immune infiltration level of NK cells quantified by MCPCOUNTER algorithm; D: Identification of NK cell related genes.

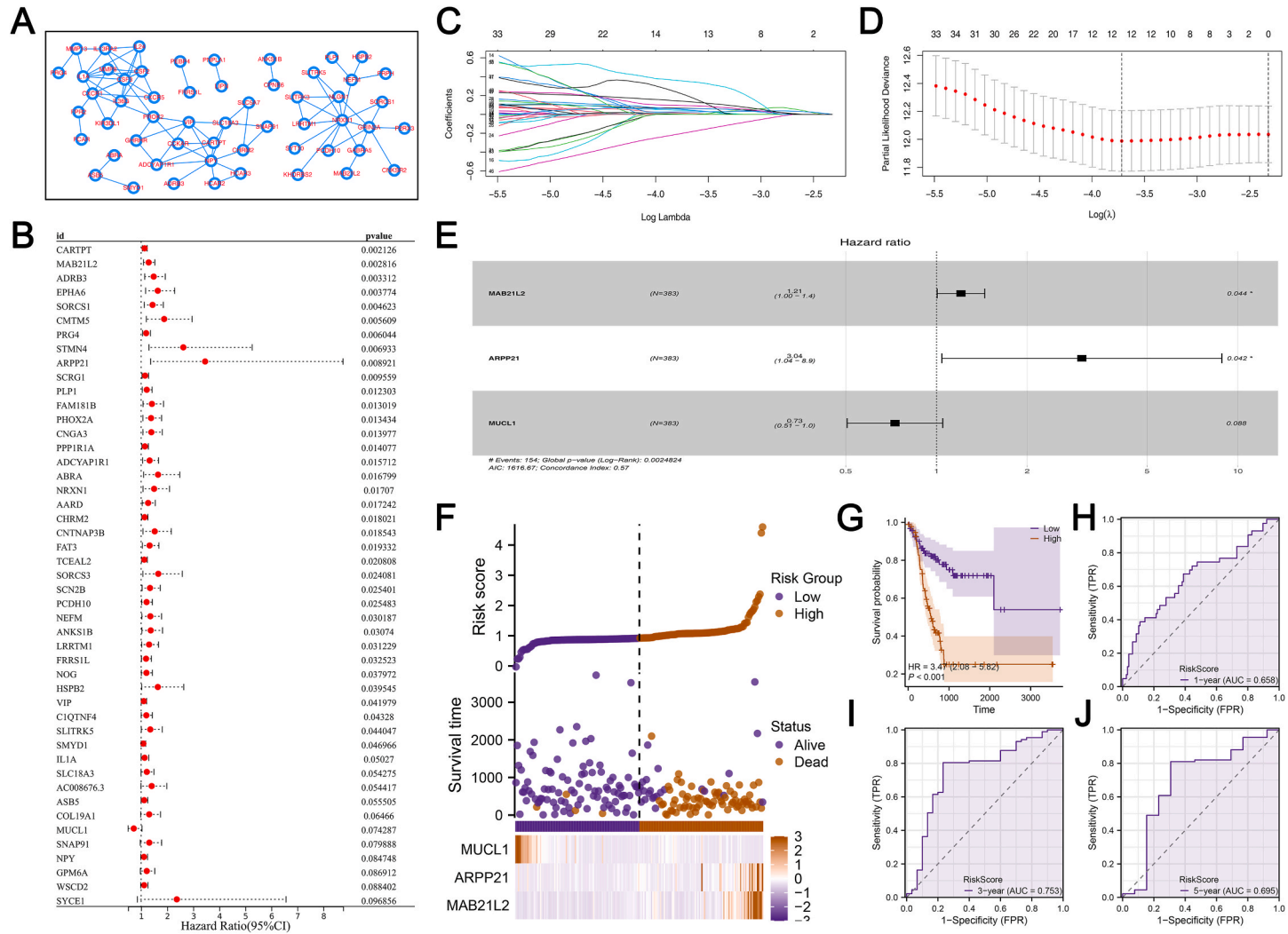
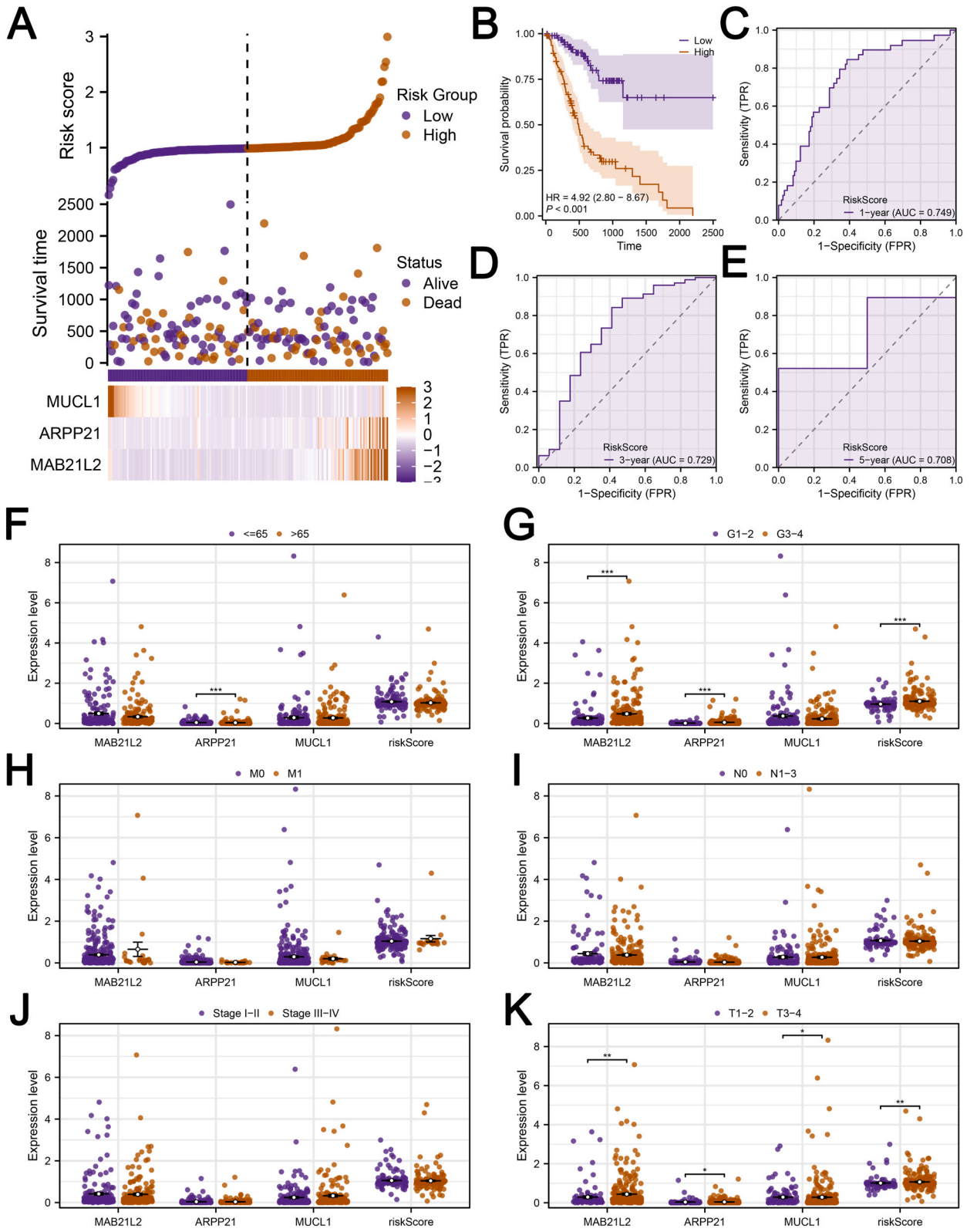


Fig. 3. Prognosis analysis of NK cell-related molecules.

Notes: **A:** PPI network of NK cell-related molecules; **B:** Univariate Cox regression analysis of NK cell-related molecules; **C-D:** LASSO regression analysis; **E:** Multivariate Cox regression analysis was performed for model construction; **F:** Overview of prognosis model in the training cohort; **G:** KM survival curves of patients in high- and low-risk group (training cohort, overall survival); **H-J:** ROC curves of 1-, 3- and 5-years survival (training cohort).



(caption on next page)

Fig. 4. Evaluation of prognosis model.

Notes: **A:** Overview of prognosis model in the validation cohort; **B:** KM survival curves of patients in high- and low-risk group (validation cohort, overall survival); **C-E:** ROC curves of 1-, 3- and 5-years survival (validation cohort); **F-K:** The clinical correlation of risk score and model molecules in gastric cancer.

modeling, and data visualization. A p-value threshold of 0.05 was considered statistically significant. However, in certain circumstances, particularly when conducting multiple testing corrections, more rigorous criteria were applied.

3. Results

3.1. Identification of genes associated with NK-cells

Fig. 1 presents the complete flowchart of this study's methodology. Based on the algorithms described above, we quantified the tumor microenvironment of gastric cancer (Fig. 2A). Several algorithms, including CIBERSORT, EPIC, MCPOUNTER, QUANTISEQ, and XCELL, were able to quantify the infiltration level of NK cells. Since CIBERSORT-identified "NK cell activated" and MCPOUNTER-identified "NK cell" exhibited relatively high infiltration scores (Fig. 2B–C), we performed differential expression analysis between patients with high and low infiltration levels for these specific NK cell populations. Fig. 2D shows that patients with high infiltration of either "NK cell activated" (identified by CIBERSORT) or "NK cell" (identified by MCPOUNTER) exhibited significant upregulation of 22 molecules and significant downregulation of 72 molecules. The protein-protein interaction network for these differentially expressed molecules is shown in Fig. 3A.

3.2. Development of a predictive model utilizing molecules associated with NK cells

To identify molecules associated with patient survival, we first conducted univariate Cox regression analysis in the training cohort, selecting factors with a p-value less than 0.1 (Fig. 3B). To reduce the dimensionality of the data and address potential multicollinearity, we subsequently performed LASSO regression analysis (Fig. 3C–D). Finally, a multivariate Cox regression analysis was conducted using the molecules identified by LASSO regression. This approach allowed us to identify a three-gene signature: *MAB21L2*, *ARPP21*, and *MUCL1*, for model construction. The risk score was calculated using the following formula: Risk score = $MAB21L2 * 0.187 + ARPP21 * 1.111 + MUCL1 * -0.318$ (Fig. 3E). As shown in Fig. 3F, the model demonstrated a higher proportion of deceased patients within the high-risk group in the training cohort. Furthermore, Kaplan-Meier survival curves revealed that patients classified as high-risk exhibited significantly poorer survival outcomes (Fig. 3G, HR = 3.47, $p < 0.001$). Finally, ROC curves demonstrated good predictive performance for patient survival (Fig. 3H–J), with 1-year, 3-year, and 5-year AUC values of 0.658, 0.753, and 0.695, respectively.

3.3. Evaluation of prognosis model and clinical correlation

We then evaluated the effectiveness of our prognostic model in the validation group (Fig. 4A). In line with the training cohort, Kaplan-Meier survival curves for the validation group showed that high-risk patients had worse prognostic outcomes (Fig. 4B). ROC curves further confirmed the model's satisfactory ability to predict patient survival (Fig. 4C–E), with 1-year, 3-year, and 5-year AUC values of 0.749, 0.729, and 0.708, respectively. Next, we investigated potential clinical correlations between the identified genes and risk scores. Analysis revealed that younger patients had higher ARPP21 expression levels (Fig. 4F). Additionally, patients with advanced tumor grade (G3-4) exhibited significantly higher levels of *MAB21L2*, *ARPP21*, and risk score compared to those with lower grades (Fig. 4G). Interestingly, no significant differences were observed in the expression levels of the model genes or risk score between patients with different metastasis stages (M0 vs. M1) or lymph node involvement (N0 vs. N1-3) (Fig. 4H & I). Similarly, no significant distinctions were found between stage I-II and stage III-IV patients (Fig. 4J). However, patients with advanced tumor stage (T3-4) displayed higher *MAB21L2*, *ARPP21*, and risk score levels while exhibiting lower *MUCL1* expression (Fig. 4K).

3.4. Biological enrichment analysis

Subsequent differential expression analysis was carried out to determine genes that were distinctly expressed between high- and low-risk patients (Fig. 5A). ClueGO analysis revealed that these DEGs were primarily enriched in biological processes such as positive regulation of synapse assembly, cognition, multicellular organismal response to stress, cAMP-mediated signaling, regulation of amine transport, and regulation of respiratory gaseous exchange (Fig. 5B). Furthermore, GSEA analysis using the Hallmark gene set identified upregulated pathways associated with myogenesis and pancreatic beta cells, while cholesterol homeostasis and MYC target pathways were downregulated in the high-risk patient group (Fig. 5C). Similarly, GSEA analysis based on GO and KEGG revealed pathways involved in angiotensin-activated signaling, noradrenergic neuron differentiation, retrograde *trans*-synaptic signaling, calcium signaling pathway, nod like receptor signaling pathway and protein export in high-risk patients (Fig. 5D–E).

3.5. Immune status and immunotherapy

Using the Estimate package, analysis showed a positive correlation between the risk score and the immune score, stromal score, and

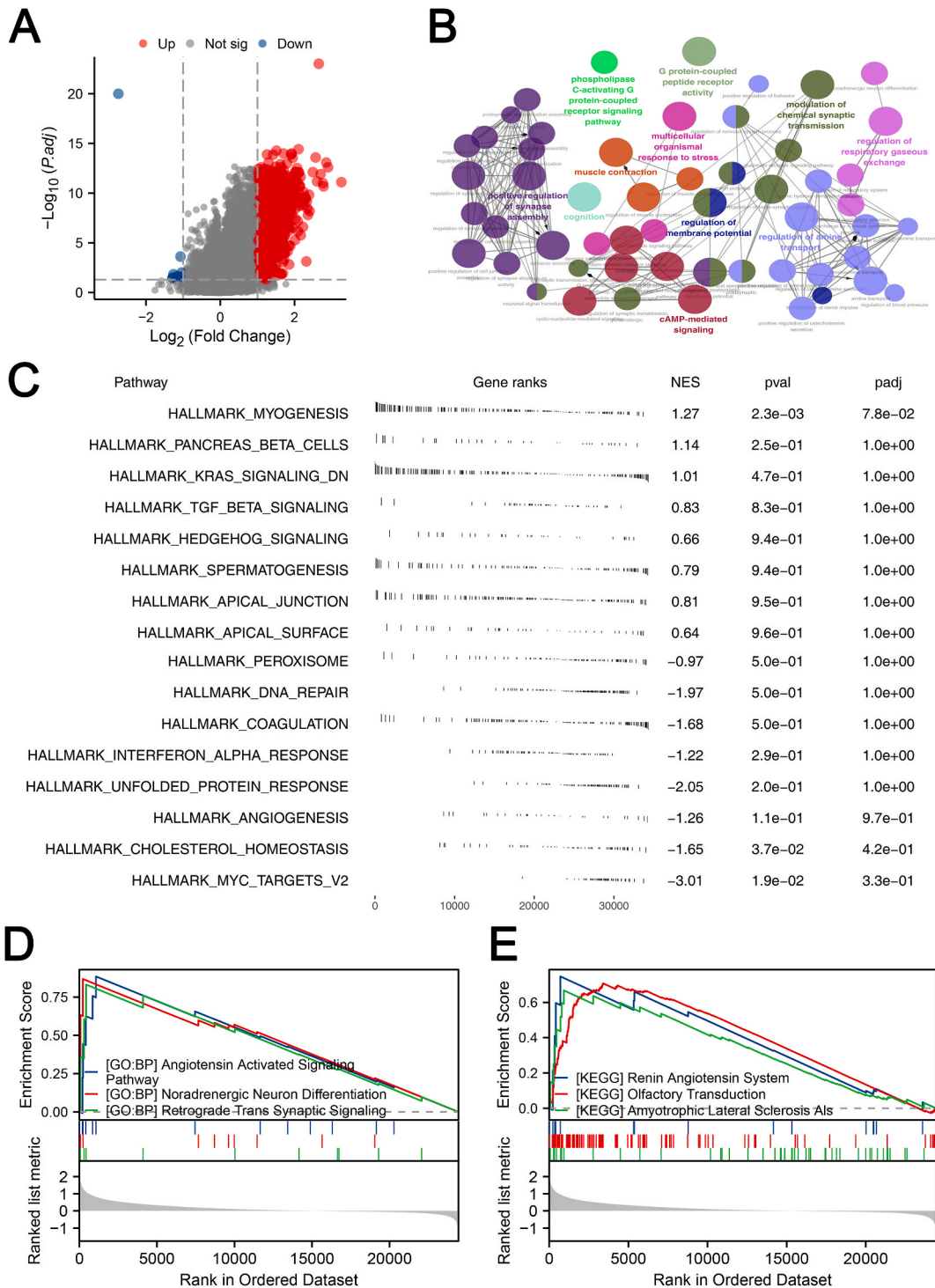


Fig. 5. Biological enrichment analysis of risk score.

Notes: **A:** DEGs analysis was performed in high- and low-risk patients; **B:** ClueGO analysis of identified DEGs; **C:** GSEA analysis was performed based on Hallmark gene set; **D:** GSEA analysis was performed based on GO gene set; **E:** GSEA analysis was performed based on KEGG gene set.

estimate score (Fig. 6A–C), indicating a substantial variation in the tumor microenvironment between high-risk and low-risk patients. Furthermore, high-risk patients displayed increased activity in their type II interferon (IFN) response (Fig. 6D). Furthermore, variations in the expression of several immune checkpoint genes were observed between high- and low-risk patients (Fig. 6E). TIDE analysis demonstrated a positive correlation between risk score and immune dysfunction, immune exclusion, and the overall TIDE score

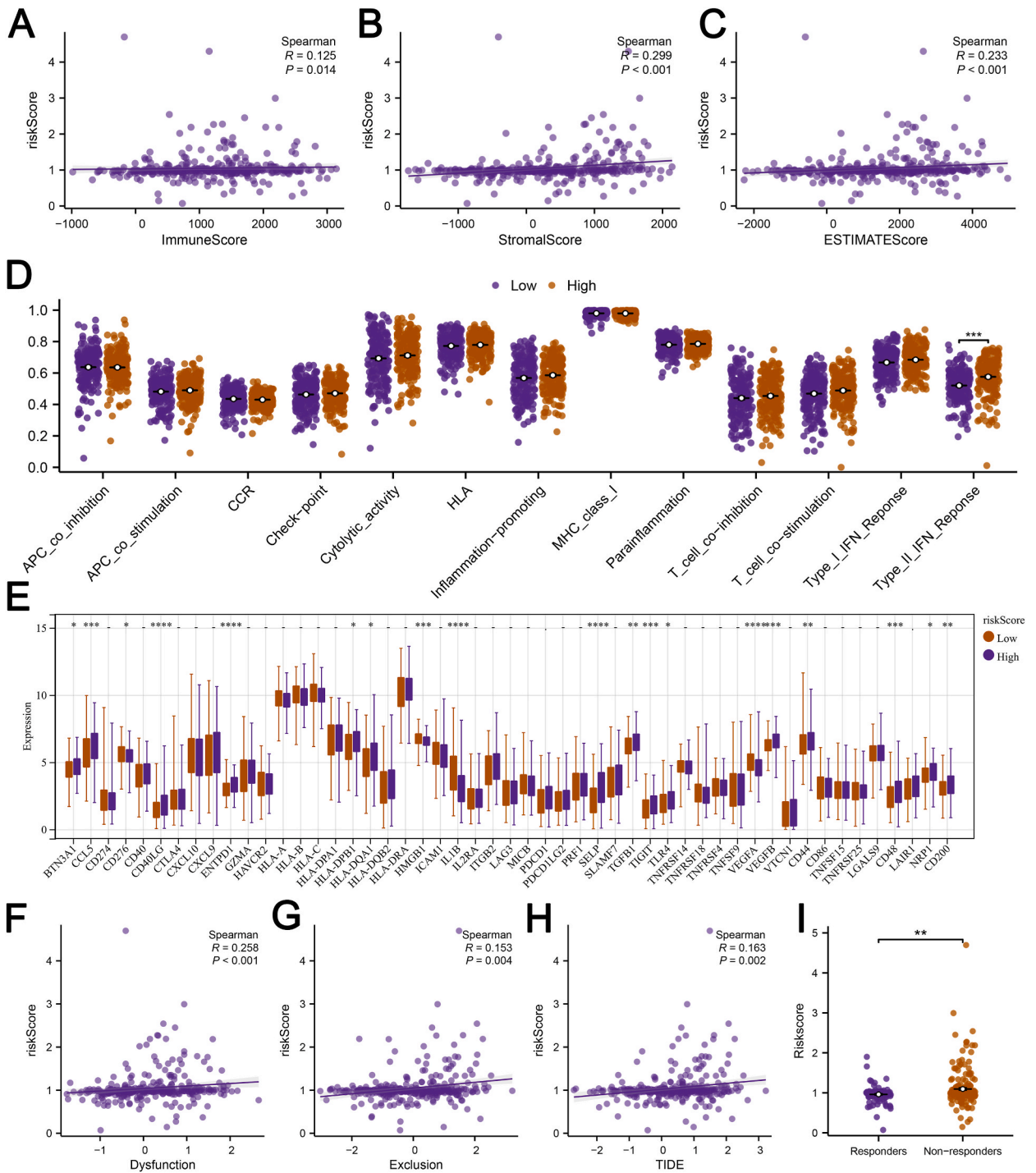


Fig. 6. Immune related analysis.

Notes: A-C: Correlation of risk score and tumor microenvironment score quantified by estimate package; D: Immune status difference in high- and low-risk patients; E: The expression level of immune checkpoints in high- and low-risk patients; F: Correlation between risk score and immune dysfunction; G: Correlation between risk score and immune exclusion; H: Correlation between risk score and TIDE score; I: Level of risk score in immune responders and non-responders.

(Fig. 6F–H). Specifically, a significant correlation was observed between risk score and dysfunction ($cor = 0.258$, $P < 0.001$), exclusion ($cor = 0.153$, $P = 0.004$), and TIDE score ($cor = 0.163$, $P = 0.002$). Additionally, patients classified as non-responders to immunotherapy tended to have higher risk scores (Fig. 6I).

3.6. Drug sensitivity and nomogram plot

We further investigated potential therapeutic vulnerabilities by performing a drug susceptibility analysis, comparing patients at high and low risk (Fig. 7A). This analysis revealed that patients classified as high-risk may exhibit greater sensitivity to axitinib, suggesting a potential therapeutic target for this patient subgroup. To facilitate individualized risk prediction, we constructed a nomogram incorporating the risk score along with relevant clinical characteristics (Fig. 7B). The calibration curves presented in Fig. 7C demonstrate a good concordance between the observed survival outcomes and those predicted by the nomogram, suggesting a reliable model for clinical application.

3.7. Further exploration of MUCL1 in gastric cancer

While MUCL1's role in other cancers has been documented [34,35], its function in gastric cancer remains unclear. Given this knowledge gap, we selected MUCL1 for further investigation. Pan-cancer analysis revealed differential expression of MUCL1 across

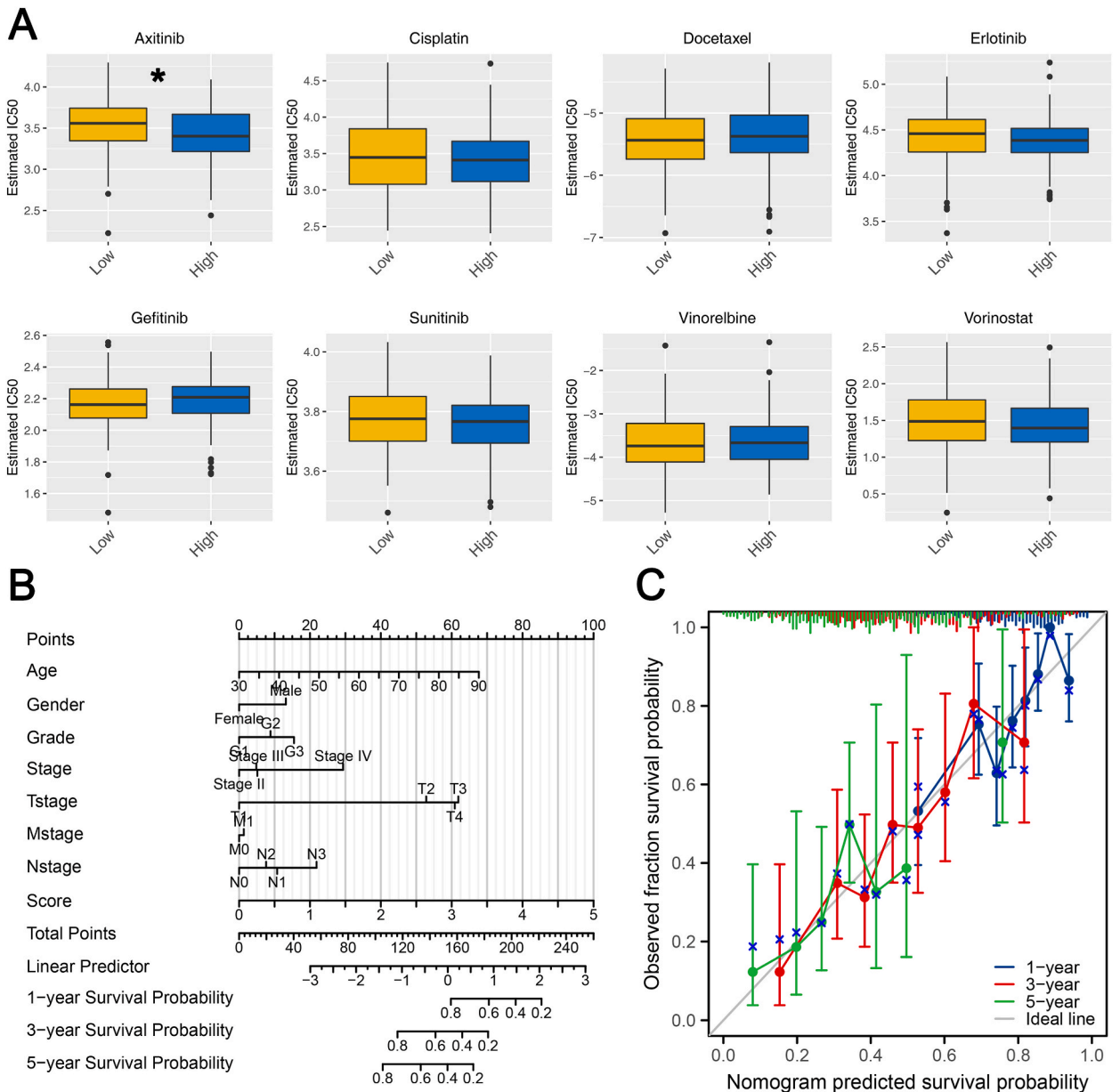


Fig. 7. Drug sensitivity analysis and nomogram plot.

Notes: A: Drug sensitivity analysis; B: Nomogram plot was constructed by combining risk score and clinical features; C: Calibration curves.

various cancer types, suggesting its potential involvement in common mechanisms of cancer development (Fig. 8A). Interestingly, our data showed upregulation of MUCL1 in both gastric cancer tissues and paired adjacent non-tumor tissues compared to controls (Fig. 8B–C). Single-cell analysis identified monocytes/macrophages and dendritic cells (DCs) as the primary cell types expressing MUCL1 within the tumor microenvironment (Fig. 8D–E). However, the HPA database indicated a decrease in MUCL1 protein

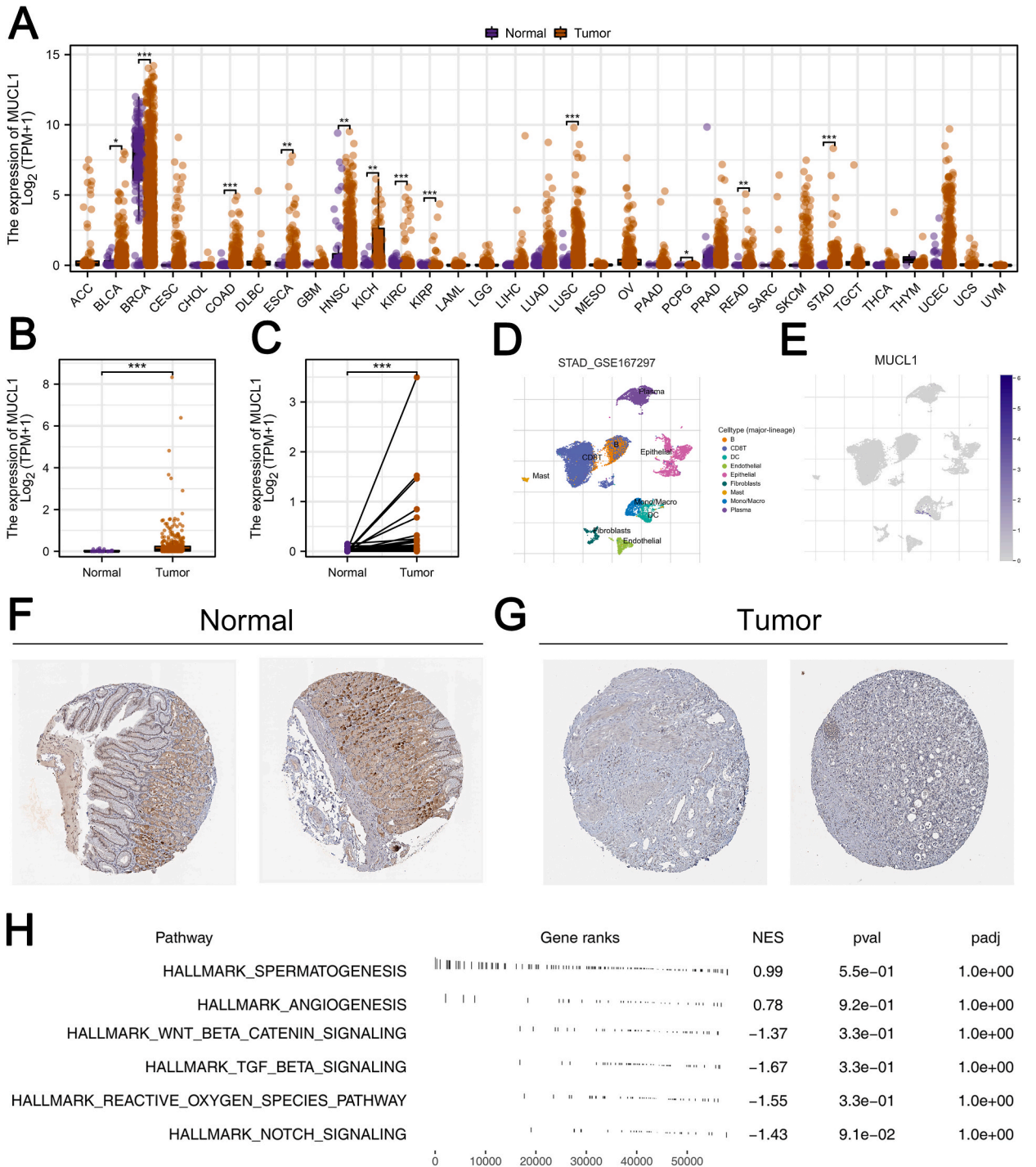


Fig. 8. Further exploration of MUCL1 in gastric cancer.

Notes: **A:** Pan-cancer analysis of MUCL1; **B–C:** Expression level of MUCL1 in gastric cancer tissue (paired and no-paired); **D–E:** Single-cell analysis of MUCL1 in gastric cancer microenvironment; **F:** The representative IHC image of MUCL1 in gastric cancer tissue; **G:** The representative IHC image of MUCL1 in normal gastric tissue; **H:** GSEA analysis of MUCL1 in gastric cancer based on Hallmark gene set.

expression within gastric cancer tissues compared to normal tissues (Fig. 8F–G). Furthermore, GSEA analysis using the Hallmark gene set revealed upregulation of spermatogenesis and angiogenesis pathways in the high-risk patient group (Fig. 8H).

3.8. MUCL1 promotes gastric cancer proliferation and migration ability

Further, we sought to investigate the role of MUCL1 in gastric cancer cells by evaluating its expression levels across different cell lines. We observed that the expression pattern of MUCL1 in gastric cancer cells is inconsistent. Specifically, compared to GES-1, both

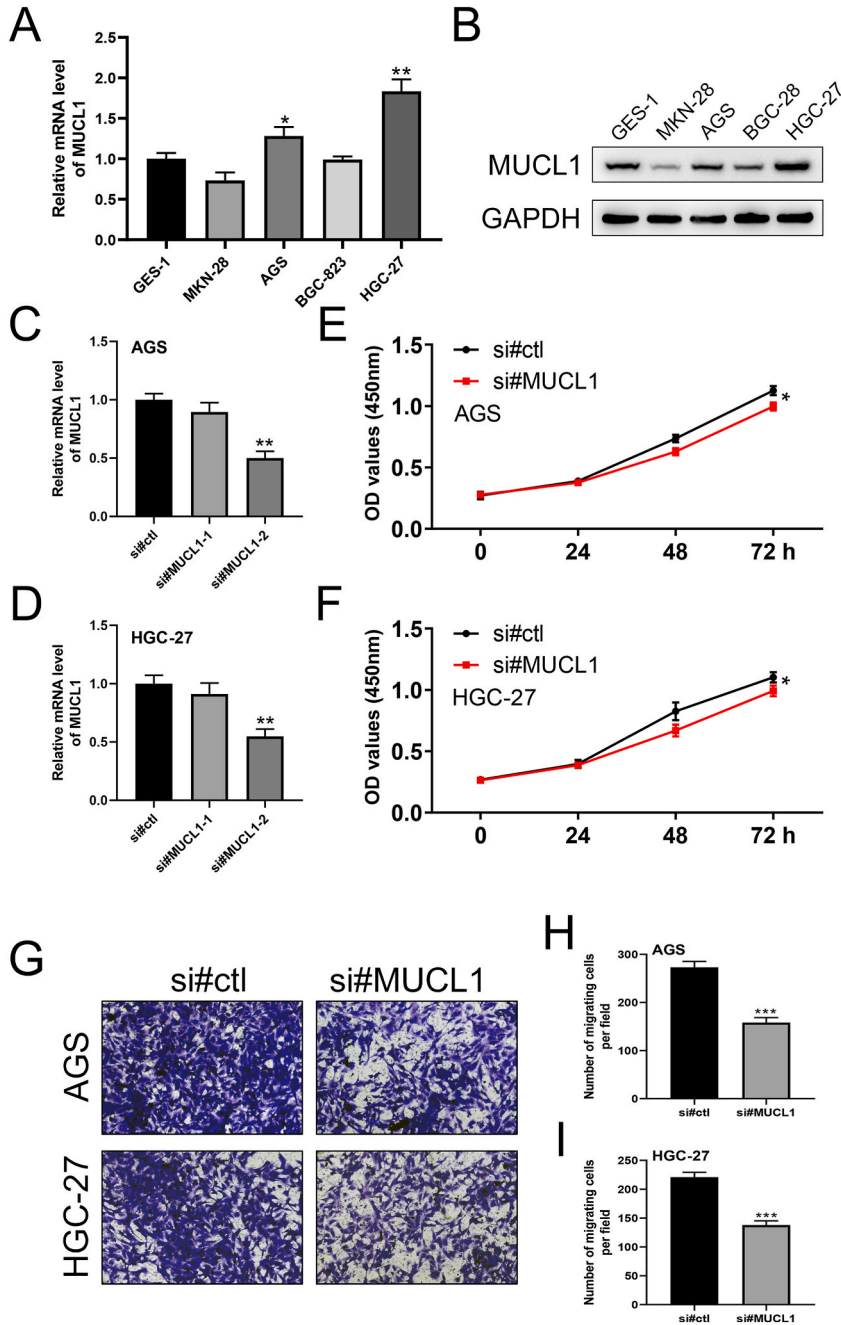


Fig. 9. MUCL1 promotes gastric cancer proliferation and migration ability.

Notes: A: The RNA level of MUCL1 in the different gastric cancer cells and normal GES-1 cell; B: The protein level of MUCL1 in the different gastric cancer cells and normal GES-1 cell (The full, non-adjusted images was shown in Supplementary Figure); C-D: The knockdown efficiency of MUCL1 in AGS and HGC-27 cells; E-F: CCK8 assay was performed in control and cells with MUCL1 knockdown; G-I: Transwell assay was performed in control and cells with MUCL1 knockdown.

AGS and HGC-27 cell lines exhibited high levels of MUCL1 expression, whereas there was no significant difference between MKN-28 and BGC-83 (Fig. 9A–B). Subsequently, we achieved knockdown of MUCL1 using siRNA transfection, with siRNA#2 showing the highest knockdown efficiency in AGS and HGC-27 cells (Fig. 9C–D). A CCK-8 assay demonstrated that MUCL1 knockdown significantly reduces the proliferation and migration capabilities of gastric cancer cells (Fig. 9E–G).

4. Discussion

Gastric malignancy, also referred to as gastric cancer, is a global health concern with a high mortality rate [36]. It arises from the lining cells of the stomach and progresses through uncontrolled growth. Early stages of gastric cancer often present with minimal or no symptoms. By the time patients experience symptoms such as indigestion, abdominal discomfort or pain, weight loss, and others, the disease may have already advanced [37]. Several risk factors contribute to gastric cancer development, including chronic gastritis, smoking, excessive consumption of pickled foods, and a family history of the disease [38]. While advancements in screening and treatment modalities have been made in recent years, early detection and preventive measures remain crucial, as most patients are diagnosed at advanced stages [39].

Natural killer cells, a crucial component of the human immune system, are cytotoxic lymphocytes with the capacity to directly eliminate infected and tumor cells [40]. Their ability to interact with tumor cells has garnered significant interest in cancer research, particularly within the field of gastric cancer [41]. Studies have revealed that the function of NK cells is often suppressed in gastric cancer patients, potentially due to alterations in the tumor microenvironment [42]. This suppression, along with a decrease in NK cell number, may be associated with tumor progression and poorer prognosis. Additionally, some cancer cells can evade detection and elimination by NK cells, contributing to gastric cancer development and metastasis [43]. In recent years, NK cell-based immunotherapy has emerged as a promising therapeutic approach for cancer [44]. By enhancing the function or quantity of NK cells, researchers aim to develop novel treatment strategies for gastric cancer patients. Overall, NK cells play a critical role in gastric cancer research, and the exploration of their interaction with tumors and potential for immunotherapy remains an active area of investigation.

In this study, we employed multiple algorithms to quantify the tumor microenvironment of gastric cancer. Differential expression analysis identified NK cell-related genes. Based on these genes, we constructed a prognostic model incorporating three key NK cell-related genes: *MAB21L2*, *ARPP21*, and *MUCL1*. Our model demonstrated high predictive accuracy in both the training and validation cohorts, with high-risk patients exhibiting significantly poorer survival outcomes. To elucidate the biological underpinnings of the risk stratification, we performed analyses focused on biological enrichment and immune-related factors. Furthermore, we observed a correlation between higher risk scores and non-responsiveness to treatment, while high-risk patients may exhibit greater sensitivity to axitinib. Following up on the model gene *MUCL1*, we found that its mRNA level was upregulated in both gastric cancer tissues and paired adjacent non-tumor tissues. However, the HPA database indicated a decrease in *MUCL1* protein expression within gastric cancer tissues compared to normal tissues. This discrepancy warrants further investigation.

MUCL1, a small glycoprotein, has emerged as a molecule of interest in recent years, particularly in cancer research [45]. In this context, *MUCL1* has been linked to tumor aggressiveness, metastatic potential, and response to anti-cancer drugs. For instance, Conley et al. demonstrated that *MUCL1* plays a critical role in breast cancer progression by regulating the FAK/JNK pathway [46]. Beyond its association with cancer biology, *MUCL1* is also being explored as a potential therapeutic target. Collectively, these findings highlight the significant biological and therapeutic relevance of *MUCL1* in cancer research. However, further in-depth studies are needed to elucidate its specific mechanisms of action within cancer and its potential interactions with other factors.

Our study highlights the critical role of NK cells in both gastric cancer progression and potential therapeutic strategies. It also paves the way for the integration of immunological parameters into prognostic models and treatment decisions. The identification of NK cell-related genes as prognostic markers, including *MAB21L2*, *ARPP21*, and *MUCL1*, underscores the complex interplay between the immune system and tumor biology, offering a promising avenue for future research. Furthermore, our findings suggest that enhancing NK cell activity could be a viable therapeutic approach, potentially leading to a paradigm shift in gastric cancer treatment. The development of this prognostic model represents a significant step towards personalized medicine in oncology. Moving forward, our research trajectory will focus on validating these markers in clinical trials, elucidating the mechanisms underlying their interaction with gastric cancer, and ultimately translating these insights into the development of targeted and immune-based therapies. The ever-evolving field of gastric cancer research holds immense promise for breakthroughs that could significantly improve patient outcomes. This emphasizes the importance of continued investigation into the tumor microenvironment and immune modulation strategies.

The interpretation and application of our results are influenced by several limitations of this study. Firstly, the dataset used in this research was sourced exclusively from publicly available databases, primarily consisting of samples from Western populations. This reliance on a specific demographic may introduce biases due to biological variations across different ethnicities, potentially limiting the generalizability of our conclusions to global populations. Secondly, bioinformatics algorithms are a powerful tool for analyzing complex genetic data. However, the results they generate are simulations of biological reality, not direct observations. As such, these computational predictions must be interpreted with caution, acknowledging that they may not fully reflect the intricate dynamics of a living system. Thirdly, the insights gained from our analyses, though promising, require further experimental validation. Such validation is crucial to confirm our observations and verify their applicability in a real-world biological context, ensuring the reliability and relevance of our findings. Lastly, while this study provides valuable insights into the role of *MUCL1* in gastric cancer, specifically its influence on cell proliferation and migration, we acknowledge certain limitations. One significant limitation is our inability to directly investigate the function of *MUCL1* within NK cells. This was due primarily to the constraints of our available experimental models and resources. Consequently, our findings on *MUCL1* are confined to its expression and functional implications in gastric cancer cell lines. Future studies utilizing comprehensive immunological assays and NK cell-specific models are required to fully

understand the role of MUCL1 in the immune aspects of gastric cancer. Addressing this gap could provide a more complete picture of MUCL1's biological functions and its potential as a therapeutic target. Addressing these limitations through future research will be essential for advancing our understanding of gastric cancer and improving patient outcomes.

Funding

This study was supported by the Science and Technology Development Fund of Shanghai Pudong New Area (Grant No: PKJ2021-Y38). This study was funded by the Pudong New Area Clinical Characteristic Discipline Project (Grant No. PWYts2021-11). This study was supported by the Discipline Construction Promoting Project of Shanghai Pudong Hospital (Grant No: Tszk2020-03, Tszb2023-06, Tszb2023-01, Zdzk2020-10).

Availability of data and materials

The datasets used and/or analyzed during the current study available from the corresponding author on reasonable request.

CRedit authorship contribution statement

Yuqin Li: Writing – original draft, Visualization, Software, Resources, Project administration, Formal analysis. **Dejun Wu:** Methodology, Formal analysis, Data curation, Conceptualization. **Anjun Xu:** Writing – original draft, Visualization, Methodology, Investigation, Formal analysis. **Ming Xu:** Validation, Software, Resources, Project administration, Methodology, Formal analysis. **Baiqing Fu:** Resources, Project administration, Methodology, Data curation. **Wujun Xiong:** Writing – original draft, Software, Methodology, Investigation, Funding acquisition, Formal analysis, Data curation, Conceptualization.

Declaration of competing interest

The authors declare that they have no known competing financial interests or personal relationships that could have appeared to influence the work reported in this paper.

Acknowledgment

None.

Appendix A. Supplementary data

Supplementary data to this article can be found online at <https://doi.org/10.1016/j.heliyon.2024.e33759>.

References

- [1] E.C. Smyth, M. Nilsson, H.I. Grabsch, N.C. van Grieken, F. Lordick, Gastric cancer, *Lancet (London, England)* 396 (10251) (2020) 635–648.
- [2] P. Karimi, F. Islami, S. Anandasabapathy, N.D. Freedman, F. Kamangar, Gastric cancer: descriptive epidemiology, risk factors, screening, and prevention, *Cancer Epidemiol. Biomarkers Prev. : a publication of the American Association for Cancer Research, cosponsored by the American Society of Preventive Oncology* 23 (5) (2014) 700–713.
- [3] A. Rizzo, V. Mollica, A.D. Ricci, I. Maggio, M. Massucci, F.L. Rojas Limpe, F.D. Fabio, A. Ardizzoni, Third- and later-line treatment in advanced or metastatic gastric cancer: a systematic review and meta-analysis, *Future oncology (London, England)* 16 (2) (2020) 4409–4418.
- [4] Z. Tan, Recent advances in the surgical treatment of advanced gastric cancer: a review, *Med. Sci. Mon. Int. Med. J. Exp. Clin. Res. : international medical journal of experimental and clinical research* 25 (2019) 3537–3541.
- [5] S.S. Joshi, B.D. Badgwell, Current treatment and recent progress in gastric cancer, *CA: a cancer journal for clinicians* 71 (3) (2021) 264–279.
- [6] A. Kawazoe, T. Ando, H. Hosaka, J. Fujita, K. Koeda, K. Nishikawa, K. Amagai, K. Fujitani, K. Ogata, K. Watanabe, et al., Safety and activity of trifluridine/tipiracil and ramucirumab in previously treated advanced gastric cancer: an open-label, single-arm, phase 2 trial, *The lancet Gastroenterology & hepatology* 6 (3) (2021) 209–217.
- [7] A.D. Ricci, A. Rizzo, F.L. Rojas Llimpe, F. Di Fabio, D. De Biase, K. Rihawi, Novel HER2-directed treatments in advanced gastric carcinoma: Another paradigm shift? *Cancers* 13 (7) (2021).
- [8] A.D. Ricci, A. Rizzo, G. Brandi, DNA damage response alterations in gastric cancer: knocking down a new wall, *Future oncology (London, England)* 17 (8) (2021) 865–868.
- [9] V. Mollica, A. Rizzo, A. Marchetti, V. Tateo, E. Tassinari, M. Rosellini, R. Massafra, M. Santoni, F. Massari, The impact of ECOG performance status on efficacy of immunotherapy and immune-based combinations in cancer patients: the MOUSEION-06 study, *Clin. Exp. Med.* 23 (8) (2023) 5039–5049.
- [10] T.H. Patel, M. Cecchini, Targeted therapies in advanced gastric cancer, *Curr. Treat. Options Oncol.* 21 (9) (2020) 70.
- [11] I. Terrén, A. Orrantia, J. Vítallé, O. Zenarruzabeitia, F. Borrego, NK cell metabolism and tumor microenvironment, *Front. Immunol.* 10 (2019) 2278.
- [12] S.Y. Wu, T. Fu, Y.Z. Jiang, Z.M. Shao, Natural killer cells in cancer biology and therapy, *Mol. Cancer* 19 (1) (2020) 120.
- [13] J.A. Myers, J.S. Miller, Exploring the NK cell platform for cancer immunotherapy, *Nat. Rev. Clin. Oncol.* 18 (2) (2021) 85–100.
- [14] H. Jiang, D. Yu, P. Yang, R. Guo, M. Kong, Y. Gao, X. Yu, X. Lu, X. Fan, Revealing the transcriptional heterogeneity of organ-specific metastasis in human gastric cancer using single-cell RNA Sequencing, *Clin. Transl. Med.* 12 (2) (2022) e730.
- [15] A. Sathe, S.M. Grimes, B.T. Lau, J. Chen, C. Suarez, R.J. Huang, G. Poultsides, H.P. Ji, Single-cell genomic characterization reveals the cellular reprogramming of the gastric tumor microenvironment, *Clin. Cancer Res. : an official journal of the American Association for Cancer Research* 26 (11) (2020) 2640–2653.

- [16] B. Han, F.Y. Mao, Y.L. Zhao, Y.P. Lv, Y.S. Teng, M. Duan, W. Chen, P. Cheng, T.T. Wang, Z.Y. Liang, et al., Altered NKp30, NKp46, NKG2D, and DNAM-1 expression on circulating NK cells is associated with tumor progression in human gastric cancer, *Journal of immunology research* 2018 (2018) 6248590.
- [17] K. Shiraishi, K. Mimura, L.F. Kua, V. Koh, L.K. Siang, S. Nakajima, H. Fujii, A. Shabbir, W.P. Yong, J. So, et al., Inhibition of MMP activity can restore NKG2D ligand expression in gastric cancer, leading to improved NK cell susceptibility, *J. Gastroenterol.* 51 (12) (2016) 1101–1111.
- [18] Y. Chen, B. Chen, T. Yang, W. Xiao, L. Qian, Y. Ding, M. Ji, X. Ge, W. Gong, Human fused NKG2D-IL-15 protein controls xenografted human gastric cancer through the recruitment and activation of NK cells, *Cell. Mol. Immunol.* 14 (3) (2017) 293–307.
- [19] P. André, C. Denis, C. Bourbon-Caillet, J. Lopez, T. Arnoux, M. Bléry, C. Bonnafous, L. Gauthier, A. Morel, et al., Anti-NKG2A mAb is a checkpoint inhibitor that promotes anti-tumor immunity by unleashing both T and NK cells, *Cell* 175 (7) (2018) 1731–1743.e1713.
- [20] M.M. Berrien-Elliott, M.T. Jacobs, T.A. Fehniger, Allogeneic natural killer cell therapy, *Blood* 141 (8) (2023) 856–868.
- [21] Z. Wang, M.A. Jensen, J.C. Zenklusen, A practical guide to the cancer genome Atlas (TCGA), *Methods Mol. Biol.* 1418 (2016) 111–141.
- [22] Y. Han, Y. Wang, X. Dong, D. Sun, Z. Liu, J. Yue, H. Wang, T. Li, C. Wang, TISCH2: expanded datasets and new tools for single-cell transcriptome analyses of the tumor microenvironment, *Nucleic Acids Res.* 51 (D1) (2023) D1425–d1431.
- [23] M. Uhlén, L. Fagerberg, B.M. Hallström, C. Lindskog, P. Oksvold, A. Mardinoglu, Å. Sivertsson, C. Kampf, E. Sjöstedt, A. Asplund, et al., Proteomics. Tissue-based map of the human proteome, *Science (New York, NY)* 347 (6220) (2015) 1260419.
- [24] B. Chen, M.S. Khodadoust, C.L. Liu, A.M. Newman, A.A. Alizadeh, Profiling tumor infiltrating immune cells with CIBERSORT, *Methods Mol. Biol.* 1711 (2018) 243–259.
- [25] J. Racle, D. Gfeller, EPIC: a tool to estimate the proportions of different cell types from bulk gene expression data, *Methods Mol. Biol.* 2120 (2020) 233–248.
- [26] E. Becht, N.A. Giraldo, L. Lacroix, B. Buttard, N. Elarouci, F. Petitprez, J. Selves, P. Laurent-Puig, C. Sautès-Fridman, W.H. Fridman, et al., Estimating the population abundance of tissue-infiltrating immune and stromal cell populations using gene expression, *Genome Biol.* 17 (1) (2016) 218.
- [27] C. Plattner, F. Finotello, D. Rieder, Deconvoluting tumor-infiltrating immune cells from RNA-seq data using quanTIseq, *Methods Enzymol.* 636 (2020) 261–285.
- [28] T. Li, J. Fan, B. Wang, N. Traugh, Q. Chen, J.S. Liu, B. Li, X.S. Liu, TIMER: a web server for comprehensive analysis of tumor-infiltrating immune cells, *Cancer Res.* 77 (21) (2017) e108–e110.
- [29] D. Aran, Z. Hu, A.J. Butte, xCell: digitally portraying the tissue cellular heterogeneity landscape, *Genome Biol.* 18 (1) (2017) 220.
- [30] G. Bindea, B. Mlecnik, H. Hackl, P. Charoentong, M. Tosolini, A. Kirilovsky, W.H. Fridman, F. Pagès, Z. Trajanoski, J. Galon, ClueGO: a Cytoscape plug-in to decipher functionally grouped gene ontology and pathway annotation networks, *Bioinformatics* 25 (8) (2009) 1091–1093.
- [31] A. Subramanian, P. Tamayo, V.K. Mootha, S. Mukherjee, B.L. Ebert, M.A. Gillette, A. Paulovich, S.L. Pomeroy, T.R. Golub, E.S. Lander, et al., Gene set enrichment analysis: a knowledge-based approach for interpreting genome-wide expression profiles, *Proc. Natl. Acad. Sci. U.S.A.* 102 (43) (2005) 15545–15550.
- [32] J. Fu, K. Li, W. Zhang, C. Wan, J. Zhang, P. Jiang, X.S. Liu, Large-scale public data reuse to model immunotherapy response and resistance, *Genome Med.* 12 (1) (2020) 21.
- [33] W. Yang, J. Soares, P. Greninger, E.J. Edelman, H. Lightfoot, S. Forbes, N. Bindal, D. Beare, J.A. Smith, I.R. Thompson, et al., Genomics of Drug Sensitivity in Cancer (GDSC): a resource for therapeutic biomarker discovery in cancer cells, *Nucleic Acids Res.* 41 (Database issue) (2013) D955–D961.
- [34] M. Abdulla, T.B. Traiki, M.A. Vaali-Mohammed, M.S. El-Wetidy, N. Alhassan, K. Al-Khayal, A. Zubaidi, O. Al-Obeed, R. Ahmad, Targeting MUCL1 protein inhibits cell proliferation and EMT by deregulating β -catenin and increases irinotecan sensitivity in colorectal cancer, *Int. J. Oncol.* 60 (3) (2022).
- [35] Q.H. Li, Z.Z. Liu, Y. Ge, X. Liu, X.D. Xie, Z.D. Zheng, Y.H. Ma, B. Liu, Small breast epithelial mucin promotes the invasion and metastasis of breast cancer cells via promoting epithelial-to-mesenchymal transition, *Oncol. Rep.* 44 (2) (2020) 509–518.
- [36] M. Venerito, A. Link, T. Rokkas, P. Malfertheiner, Gastric cancer - clinical and epidemiological aspects, *Helicobacter* 21 (Suppl 1) (2016) 39–44.
- [37] B. Kim, S.J. Cho, Endoscopic screening and surveillance for gastric cancer, *Gastrointestinal endoscopy clinics of North America* 31 (3) (2021) 489–501.
- [38] A.P. Thrift, El-Serag HB: Burden of Gastric Cancer, *Clin. Gastroenterol. Hepatol. : the official clinical practice journal of the American Gastroenterological Association* 18 (3) (2020) 534–542.
- [39] P. Petryszyn, N. Chapelle, T. Matysiak-Budnik, Gastric cancer: where are we heading? *Dig. Dis.* 38 (4) (2020) 280–285.
- [40] Y. Chen, D. Lu, A. Churov, R. Fu, Research progress on NK cell receptors and their signaling pathways, *Mediat. Inflamm.* 2020 (2020) 6437057.
- [41] H.Y. Na, Y. Park, S.K. Nam, J. Koh, Y. Kwak, S.H. Ahn, D.J. Park, H.H. Kim, K.S. Lee, H.S. Lee, Prognostic significance of natural killer cell-associated markers in gastric cancer: quantitative analysis using multiplex immunohistochemistry, *J. Transl. Med.* 19 (1) (2021) 529.
- [42] C. Guillerey, NK cells in the tumor microenvironment, *Adv. Exp. Med. Biol.* 1273 (2020) 69–90.
- [43] T. Li, Q. Zhang, Y. Jiang, J. Yu, Y. Hu, T. Mou, G. Chen, G. Li, Gastric cancer cells inhibit natural killer cell proliferation and induce apoptosis via prostaglandin E2, *Oncimmunology* 5 (2) (2016) e1069936.
- [44] P.S. Becker, G. Suck, P. Nowakowska, E. Ullrich, E. Seifried, P. Bader, T. Tonn, C. Seidl, Selection and expansion of natural killer cells for NK cell-based immunotherapy, *Cancer Immunol. Immunother.* : CII 65 (4) (2016) 477–484.
- [45] J. Navarro-Barriuso, M.J. Mansilla, B. Quirant-Sánchez, A. Ardiaca-Martínez, A. Teniente-Serra, S. Presas-Rodríguez, A. Ten Brinke, C. Ramo-Tello, E. M. Martínez-Cáceres, MAP7 and MUCL1 are biomarkers of vitamin D3-induced tolerogenic dendritic cells in multiple sclerosis patients, *Front. Immunol.* 10 (2019) 1251.
- [46] S.J. Conley, E.E. Bosco, D.A. Tice, R.E. Hollingsworth, R. Herbst, Z. Xiao, HER2 drives Mucin-like 1 to control proliferation in breast cancer cells, *Oncogene* 35 (32) (2016) 4225–4234.